JOURNAL OF CHEMICAL EDUCATION

pubs.acs.org/jchemeduc Communication

The Briggs–Rauscher Reaction: A Demonstration of Sequential Spatiotemporal Patterns

Zhuoxuan Li, Ling Yuan,* Mengfei Liu, Zhenfang Cheng, Juhua Zheng, Irving R. Epstein, and Qingyu Gao*

Cite This: https://dx.doi.org/10.1021/acs.jchemed.0c00892 Read Online

ACCESS | Metrics & More | Article Recommendations | Supporting Information

ABSTRACT: The Briggs–Rauscher reaction is a popular demonstration to illustrate chemical oscillations in laboratories, classrooms, and public seminars because of its simplicity and visual appeal. Here, we adapt the Briggs–Rauscher reaction to present reaction–diffusion–convection patterns in the undergraduate general or physical chemistry laboratory. By maintaining the ratio between malonic acid and potassium iodate concentrations as 0.2 in an uncovered Petri dish, sequential patterns (transient dendritic patterns and rotating dendritic patterns) can be observed, which are induced by the interaction of reaction, diffusion, and convection. This beautiful demonstration captures students' attention and inspires reflection and discussion about similar phenomena in nature as well as the wealth of behaviors in systems far from equilibrium.

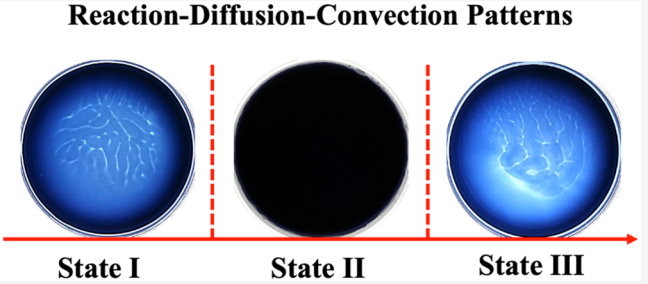

KEYWORDS: *First-Year Undergraduate/General Chemistry, Second-Year Undergraduate, Physical Chemistry, Kinetics, Oxidation/Reduction*

INTRODUCTION

Students are fascinated by experiments involving redox or other reactions that exhibit color changes and pattern formation. Oscillatory chemical systems, such as the well-known Belousov–Zhabotinsky (BZ)[1] reaction and the Briggs–Rauscher (BR)[2] reaction, display many fascinating phenomena and frequently serve as the basis for vivid classroom demonstrations. The periodic color changes seem almost magical.[3,4] Furthermore, coupling between chemical oscillations and transport processes can generate spatial symmetry-breaking and pattern formation, such as traveling waves or patterns,[5−8] which enhance the visual and intellectual appeal and inspire students to connect their observations with similar complex spatiotemporal behaviors in nature. Moreover, chemical reactions lead to changes in physical properties, such as density, temperature, and surface tension, which may elicit hydrodynamics flows leading to new patterns.[9−13] For example, if a denser solution overlies a less dense one as a result of reaction, this density difference can trigger buoyancy-driven convection in the gravity field, which can generate traveling convective fingers, breaking the transverse symmetry in oscillatory systems.[14] In a horizontally arranged shallow liquid layer open to the atmosphere or a Hele–Shaw cell, surface tension and density gradients induced by reaction may also contribute to pattern formation.[15−17] In the excitable BZ reaction system, segmentation waves have been obtained from the interaction of Marangoni (surface tension-driven) and buoyancy-driven flows.[9]

Unfortunately, for the purpose of hands-on classroom or laboratory experiments, the BZ reaction system requires about 1 M H_2SO_4 or HNO_3 and expensive metal catalysts (Ru^{2+}, Ce^{3+}, or $[Fe(phen)_3]^{2+}$). The BR reaction, in contrast, only needs 0.2 M H_2SO_4 and relatively inexpensive Mn^{2+}, and it exhibits more dramatic cyclic color changes than the BZ system, from colorless to yellow to blue. It has been used as a lecture and laboratory demonstration of temporal oscillations for over three decades.[1,18] The final state of the BR reaction depends primarily on the ratio, R, of the malonic acid (MA) and iodate concentrations. If $R \ll 2$, the reaction produces a large amount of iodine, which results in surface tension changes, leading to Marangoni flows.[11,19] Such flows may couple with reaction and diffusion to yield a rich array of spatiotemporal patterns.

Here, we describe a chemical demonstration of reaction–diffusion–convection patterns in the typical BR reaction system. The experiment clearly illustrates that changes in density and surface tension during the reaction significantly affect the

Received: July 2, 2020
Revised: November 5, 2020

pattern formation. We suggest that it is valuable to introduce these topics in the physical chemistry lab, allowing a simple macroscopic observation to reveal kinetic information and the importance of convective motion.

MATERIALS

Analytical reagent hydrogen peroxide, manganese sulfate, sulfuric acid, malonic acid ($CH_2(COOH)_2$, MA), starch, and potassium iodate (Sinopharm Chemical Regents) are used without purification and prepared with deionized water (Millipore, ELIX 5). The BR solutions are prepared as follows:

- Hydrogen peroxide (3.579 M, 100 mL) is prepared by diluting hydrogen peroxide 30% solution (CAS 7722-84-1) and titrated with standard potassium permanganate.
- Dilute sulfuric acid (0.200 M, 100 mL) can be prepared by diluting 1 M sulfuric acid.
- 0.5% starch indicator solution (100 mL) is prepared from 0.5 g of soluble starch (CAS 9005-84-9).
- A manganese sulfate solution (0.005 M, 100 mL) is prepared from 0.08451 g of analytical reagent manganese sulfate monohydrate (CAS 10034-96-5).
- A potassium iodate solution (0.150 M, 100 mL) is prepared from 3.210 g of analytical reagent potassium iodate (CAS 7758-05-6). A magnetic stirrer can be used to accelerate the dissolution of potassium iodate.
- A malonic acid solution (0.030 M, 100 mL) is prepared from 0.3122 g of analytical reagent malonic acid (CAS 141-82-2).

All solutions are stored at room temperature. The potassium iodate and hydrogen peroxide solution should be protected from light.

PROCEDURE

The reactor used for most of the experiments consists of a 5.5 cm diameter quartz Petri dish with a flat bottom. Experiments are performed at room temperature (about 25.0 °C). The BR solution is made by mixing the six solutions in a 50 mL beaker in the following order: $MnSO_4$ (5 mL), H_2SO_4(5 mL), MA (5 mL), KIO_3 (5 mL), H_2O_2 (10 mL), and 2 mL 0.5% starch indicator for visualizing the patterns. The desired volume of the BR solution is transferred to the reactor immediately. The temporal evolution can be recorded using a digital video camera (Canon, 70D) connected to a PC. An annular LED white source is used as a background light source at fixed intensity. The Petri dish must be clean in order to avoid accumulation of oxygen bubbles on the wall, which can influence the pattern formation.

HAZARDS

Hydrogen peroxide solutions (3.579 M) are prepared from 30% hydrogen peroxide, which can cause skin and eye irritation on contact, and abdominal pain if ingested. The 0.2 M sulfuric acid may cause harm to the eyes or skin and is harmful to the digestive system if ingested. Dilute product solutions of iodide/iodine may stain the skin. The chemicals manganese sulfate, iodate, and malonic acid are hazardous in powder form, so the solutions should be prepared by the instructor. Splash goggles and rubber gloves should be worn when handling the chemicals. The waste liquid and materials should be disposed of in accordance with institutional guidelines.

DISCUSSION

The oscillatory decomposition of hydrogen peroxide in acid media in the presence of iodate is known as the Bray−Liebhafsky (BL) reaction,[20] which can be written formally as two processes:

$$2IO_3^- + 5H_2O_2 + 2H^+ \rightarrow I_2 + 5O_2 + 6H_2O \quad \text{(R1)}$$

$$I_2 + 5H_2O_2 \rightarrow 2H^+ + 2IO_3^- + 4H_2O \quad \text{(R2)}$$

The essential process in both the BL and BR reactions is the oscillatory decomposition of hydrogen peroxide. They differ in that the main iodine consumption process in the BL reaction is oxidation by hydrogen peroxide, whereas in the BR reaction the iodine is consumed by both hydrogen peroxide (eq R2) and malonic acid (eq R3). In a homogeneous system, the BR reaction can display transient oscillations under batch conditions[18] and shows clock reaction behavior due to autocatalysis in both iodine and iodide.[21]

$$5CH_2(COOH)_2 + H^+ + IO_3^- + 2I_2 \rightarrow 5CIH(COOH)_2 + 3H_2O \quad \text{(R3)}$$

For studying the iodine pattern, we fix $R = 0.2$ in all experiments. The thickness of the solution layer, d, is varied in the range 2.0−5.0 mm. When d exceeds a threshold (2 mm), convective phenomena appear, coupled with diffusion and the nonlinear kinetics. Pattern formation exhibits three states: the dendritic pattern and front waves (state I), a high iodine state (state II), and rotating dendritic lines (state III). With a layer thickness of 3 mm, the spatiotemporal patterns (Figure 1b)

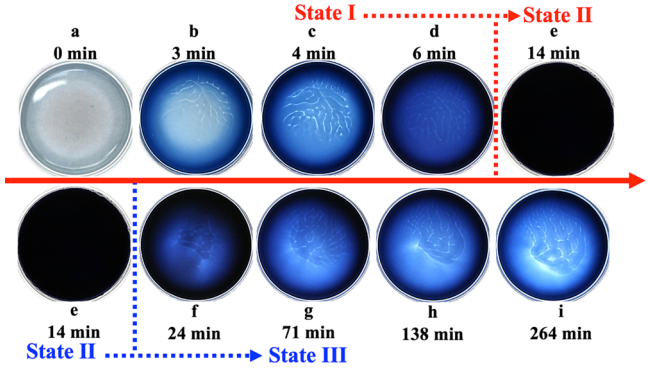

Figure 1. Evolution of spatiotemporal patterns. Layer thickness is 3.0 mm.

suddenly appear after 3 min and rapidly evolve into a dendritic pattern with inward-moving fronts (Figure 1a−c). The blue color indicates the region of high iodine concentration, while the white stripes represent low iodine concentration regions. The polyiodide ions form a complex with the starch, which decreases the effective diffusion coefficient of the polyiodide ions.[22] After 14 min, the first-stage chemo-hydrodynamic pattern disappears and gives way to another homogeneous state (state II, high iodine state, seen in Figure 1e). As the reaction proceeds, the iodine is gradually consumed by reaction with hydrogen peroxide and MA, or evaporation.[18] Then, the networked dendritic lines (state III) (Figure 1h) form and rotate periodically and spread toward the center, showing motor-like behavior. Under these conditions, the rotating networked dendritic lines in the BR system can be sustained for dozens of hours. The duration of the high iodine state and the structure of the patterns depend on the layer thickness (see videos in

https://dx.doi.org/10.1021/acs.jchemed.0c00892
J. Chem. Educ. XXXX, XXX, XXX−XXX

Supporting Information). The thicker the layer is, the longer the duration of the high iodine state is. When the layer thickness is 2 mm, the high iodine state exists only briefly. If d is increased to 3 mm, the high iodine state persists for 11 min.

To understand the origin of the patterns observed, it is useful to analyze the mechanistic origin for both BR (and BL) batch oscillations and the chemo-hydrodynamic characteristics. Batch oscillations for hydrogen peroxide decomposition are driven by HIO_2 autocatalysis.[23−25] After oscillations end, the transition from state I (low $[I_2]$ and $[I^-]$) to state II (high $[I_2]$ and $[I^-]$) occurs after a time delay at $R \ll 2$.[21,26,27] Meanwhile, I^- autocatalysis occurs via reactions (eqs R4 and R5), where X in eq R5-1 denotes the agent consuming iodine and hypoiodous acid such as water, hydrogen peroxide, malonic acid, or iodomalonic acid from eq R5-1 to eq R5-5, and Y and P are the general terms for the other products in eq R5-1 and eq R5-5, respectively.

$$6H^+ + 5I^- + IO_3^- \rightarrow 3I_2 + 3H_2O \quad \text{(R4)}$$

$$I_2 + X \rightarrow 2I^- + Y \quad \text{(R5)}$$

$$I_2 + H_2O \leftrightarrow HOI + I^- + H^+ \quad \text{(R5-1)}$$

$$HOI + H_2O_2 \rightarrow I^- + O_2 + H_2O + H^+ \quad \text{(R5-2)}$$

$$HOI + CH_2(COOH)_2 \rightarrow ClH(COOH)_2 + H_2O \quad \text{(R5-3)}$$

$$HOI + ClH(COOH)_2 \rightarrow Cl_2(COOH)_2 + H_2O \quad \text{(R5-4)}$$

$$Cl_2(COOH)_2 + H_2O_2 \xrightarrow{Mn^{2+}} 2H^+ + 2I^- + P \quad \text{(R5-5)}$$

The process in eq R5 can be decomposed into two paths: (R5-1 + R5-2) and (R5-1 + 0.5R5-3 + 0.5R5-4 + R5-5).

For explaining the three-stage patterns, a simple schematic of the chemo-hydrodynamic origins of spatiotemporal pattern formation is given in Figure 2. The coupling between iodide autocatalysis and transport (diffusion and convection) produces white dendritic patterns and inward-moving fronts. During iodide autocatalysis, acid is generated in eqs R5-1, R5-2, R5-5, promoting process R4, which generates iodine and triiodide, leading to the emergence of the second-stage state, i.e., the high iodine state. Then, the iodine is gradually consumed by reaction with hydrogen peroxide and MA, or evaporation,[18] after which the system is again dominated by iodide autocatalysis to regenerate chemo-hydrodynamic patterns, i.e., rotating networked dendritic lines.

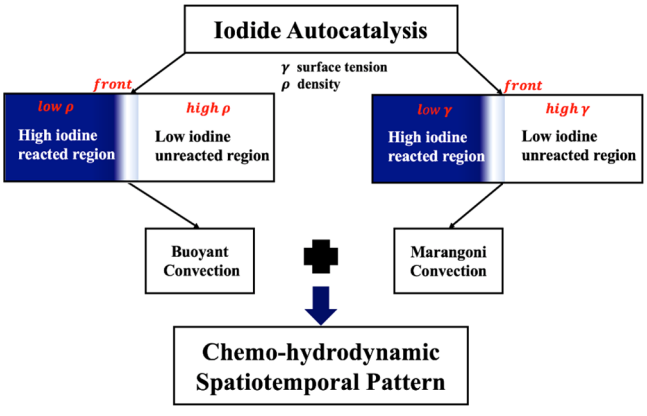

Figure 2. Schematic diagram of chemical and hydrodynamic pattern origins.

In this system, convection can be buoyancy-driven and/or Marangoni-driven.[28] The BR reaction system undergoes a temperature increase during the transition from the low iodide and iodine to the high iodide and iodine concentration state.[19] Heat accumulates in the reacting region where iodide autocatalysis occurs, causing density difference-induced buoyant convection. Also, iodine is generated in the reacted region, leading to a local decrease of the surface tension. The surface tension difference between the low iodine and high iodine regions induces additional fluid motion, known as Marangoni convection. Since high iodine concentration occurs along the edge of the Petri dish, the convective transport propels fluid toward the center of the dish, leading to rotation.

The structures seen here resemble those reported in the methylene blue−glucose reaction[17,29] and the air oxidation of vitamin C.[11,30] However, the formation mechanism of the line patterns here is quite different: the previous patterns are mainly controlled by buoyant convection. In the BR reaction system, chemo-hydrodynamic patterns involve both buoyancy and Marangoni convection simultaneously. In addition, the glucose and vitamin C reaction systems are run in semibatch media which are open with respect to O_2 but closed with respect to other species.

As the reaction proceeds, the instructor can encourage students to find the similarity between patterns in this reaction and patterns in nature and can give a brief discussion of the functions of convection and the nonlinear kinetics in the BR system, while emphasizing the importance of the system being far from equilibrium.

CONCLUSION

This article presents a demonstration of sequential patterns in the classic BR system, which can promote student interest in chemistry and enhance understanding of the common dynamics of pattern formation in chemical, physical, and living systems. Furthermore, the BR reaction uses chemicals at a mildly acidic pH, which is suitable and safe for hands-on use. Here, it is utilized to demonstrate sequential spatiotemporal self-organization and in particular to illustrate the coupling between nonlinear chemical dynamics and transport phenomena.

ASSOCIATED CONTENT

Supporting Information

The Supporting Information is available at https://pubs.acs.org/doi/10.1021/acs.jchemed.0c00892.

Video showing pattern formation with layer thickness 2 mm (AVI)

Video showing pattern formation with layer thickness 3 mm (AVI)

Video showing pattern formation with layer thickness 4 mm (AVI)

Video showing pattern formation with layer thickness 5 mm (AVI)

AUTHOR INFORMATION

Corresponding Authors

Ling Yuan − *College of Chemical Engineering, China University of Mining and Technology, Xuzhou 221116, China;*

https://dx.doi.org/10.1021/acs.jchemed.0c00892
J. Chem. Educ. XXXX, XXX, XXX−XXX

orcid.org/0000-0002-3623-113X;
Email: yuanling_1984@163.com

Qingyu Gao − *College of Chemical Engineering, China University of Mining and Technology, Xuzhou 221116, China; Department of Chemistry and Volen Center for Complex Systems, Brandeis University, Waltham, Massachusetts 02454-9110, United States;* orcid.org/0000-0002-5520-0240;
Email: gaoqy@cumt.edu.cn

Authors

Zhuoxuan Li − *College of Chemical Engineering, China University of Mining and Technology, Xuzhou 221116, China*

Mengfei Liu − *College of Chemical Engineering, China University of Mining and Technology, Xuzhou 221116, China*

Zhenfang Cheng − *College of Chemical Engineering, China University of Mining and Technology, Xuzhou 221116, China*

Juhua Zheng − *College of Chemical Engineering, China University of Mining and Technology, Xuzhou 221116, China*

Irving R. Epstein − *Department of Chemistry and Volen Center for Complex Systems, Brandeis University, Waltham, Massachusetts 02454-9110, United States;* orcid.org/0000-0003-3180-4055

Complete contact information is available at: https://pubs.acs.org/10.1021/acs.jchemed.0c00892

Notes

The authors declare no competing financial interest.

■ ACKNOWLEDGMENTS

This work was supported by Grant 21773304 from the National Natural Science Foundation of China, the Natural Science Foundation of Jiangsu Province (Grant BK20171186), and Grant CHE-1856484 from the U.S. National Science Foundation. The authors would like to thank Rui Teng for their help with video processing.

■ REFERENCES

(1) Kolb, D. Oscillating Reactions. *J. Chem. Educ.* **1988**, *65* (11), 1004.
(2) Briggs, T. S.; Rauscher, W. C. An Oscillating Iodine Clock. *J. Chem. Educ.* **1973**, *50* (7), 496.
(3) Pfennig, B. W.; Roberts, R. T. A Kinetics Demonstration Involving a Green-Red-Green Color Change Resulting from a Large-Amplitude pH Oscillation. *J. Chem. Educ.* **2006**, *83* (12), 1804−1806.
(4) Degn, H. Oscillating Chemical Reactions in Homogeneous Phase. *J. Chem. Educ.* **1972**, *49* (5), 302−307.
(5) Turing, A. M. The Chemical Basis of Morphogenesis. *Philos. Trans. R. Soc. B* **1952**, *237*, 37−72.
(6) Kovalchuk, N. M.; Vollhardt, D. Effect of Buoyancy on Appearance and Characteristics of Surface Tension Repeated Auto-Oscillations. *J. Phys. Chem. B* **2005**, *109* (31), 15037−15047.
(7) Stefan, C.; Müller Miike, H. *New Trends in Nonlinear Dynamics and Pattern-Forming Phenomena, The Geometry of Nonequilibrium*; Pierre, C., Patrick, H., Eds.; Springer: New York, 2006; pp 11−19.
(8) Horváth, J.; Szalai, I.; De Kepper, P. An Experimental Design Method Leading to Chemical Turing Patterns. *Science* **2009**, *324* (5928), 772−775.
(9) Rossi, F.; Budroni, M. A.; Marchettini, N.; Carballido-Landeira, J. Segmented Waves in a Reaction-Diffusion-Convection System. *Chaos* **2012**, *22* (3), 037109.
(10) Šebestíková, L.; Hauser, M. J. B. Buoyancy-Driven Convection may Switch between Reactive States in Three-Dimensional Chemical Waves. *Phys. Rev.E* **2012**, *85* (3), 036303.
(11) Bába, P.; Rongy, L.; De Wit, A.; Hauser, M. J. B.; Tóth, Á.; Horváth, D. Interaction of Pure Marangoni Convection with a Propagating Reactive Interface under Microgravity. *Phys. Rev. Lett.* **2018**, *121* (2), 024501.
(12) Bába, P.; Tóth, Á.; Horváth, D. Surface-Tension-Driven Dynamic Contact Line in Microgravity. *Langmuir* **2019**, *35* (2), 406−412.
(13) Inomoto, O.; Müller, S. C.; Kobayashi, R.; Hauser, M. J. B. Acceleration of Chemical Reaction Fronts. *Eur. Phys. J.: Spec. Top.* **2018**, *227* (5−6), 493−507.
(14) Escala, D. M.; Budroni, M. A.; Carballido-Landeira, J.; De Wit, A.; Munuzuri, A. P. Self-Organized Traveling Chemo-Hydrodynamic Fingers Triggered by a Chemical Oscillator. *J. Phys. Chem. Lett.* **2014**, *5* (3), 413−418.
(15) Miike, H.; Müller, S. C.; Hess, B. Oscillatory Deformation of Chemical Waves Induced by Surface Flow. *Phys. Rev. Lett.* **1988**, *61* (18), 2109−2112.
(16) Liu, Y.; Zhou, W.; Zheng, T.; Zhao, Y.; Gao, Q.; Pan, C.; Horvath, A. K. Convection-Induced Fingering Fronts in the Chlorite-Trithionate Reaction. *J. Phys. Chem. A* **2016**, *120* (16), 2514−20.
(17) Pons, A. J.; Sagués, F.; Bees, M. A.; Sørensen, P. G. Pattern Formation in the Methylene-Blue-Glucose System. *J. Phys. Chem. B* **2000**, *104* (10), 2251−2259.
(18) Furrow, S. D. A Modified Recipe and Variations for the Briggs−Rauscher Oscillating Reaction. *J. Chem. Educ.* **2012**, *89* (11), 1421−1424.
(19) Popity-Toth, E.; Potari, G.; Erdos, I.; Horváth, D.; Tóth, Á. Marangoni Instability in the Iodate-Arsenous Acid Reaction Front. *J. Chem. Phys.* **2014**, *141* (4), 044719.
(20) Bray, W. C.; Liebhafsky, H. A. Reactions Involving Hydrogen Peroxide, Iodine and Iodate Ion. *J. Am. Chem. Soc.* **1931**, *53*, 38−44.
(21) Furrow, S. D.; Cervellati, R.; Greco, E. Study of the Transition to Higher Iodide in the Malonic acid Briggs−Rauscher Oscillator. *React. Kinet., Mech. Catal.* **2016**, *118* (1), 59−71.
(22) Lengyel, I.; Epstein, I. R. Modeling of Turing Structures in the Chlorite-Iodide-Malonic Acid-Starch Reaction System. *Science* **1991**, *251* (4994), 650−652.
(23) Noyes, R. M.; Furrow, S. D. The Oscillatory Briggs-Rauscher Reaction. 3. A Skeleton Mechanism for Oscillations. *J. Am. Chem. Soc.* **1982**, *104* (1), 45−48.
(24) De Kepper, P.; Epstein, I. R. Mechanistic Study of Oscillations and Bistability in the Briggs-Rauscher Reaction. *J. Am. Chem. Soc.* **1982**, *104* (1), 49−55.
(25) Schmitz, G.; Kolar-Anic, L.; Anic, S.; Grozdic, T.; Vukojevic, V. Complex and Chaotic Oscillations in a Model for the Catalytic Hydrogen Peroxide Decomposition under Open Reactor Conditions. *J. Phys. Chem. A* **2006**, *110* (34), 10361−8.
(26) Furrow, S. D.; Cervellati, R.; Greco, E. A Study of the Cerium-Catalyzed Briggs-Rauscher Oscillating Reaction. *Z. Naturforsch., B: J. Chem. Sci.* **2012**, *67*, 89−97.
(27) Pagnacco, M. C.; Maksimovic, J. P.; Potkonjak, N. I.; Bozic, B. D.; Horváth, A. K. Transition from Low to High Iodide and Iodine Concentration States in the Briggs-Rauscher Reaction: Evidence on Crazy Clock Behavior. *J. Phys. Chem. A* **2018**, *122* (2), 482−491.
(28) Sun, Z. F.; Fahmy, M. Onset of Rayleigh-Bénard-Marangoni Convection in Gas-Liquid Mass Transfer with Two-Phase Flow: Theory. *Ind. Eng. Chem. Res.* **2006**, *45* (9), 3293−3302.
(29) Adamcíková, L. u.; Sevcík, P. The Blue Bottle Experiment-Simple Demonstration of Self-Organization. *J. Chem. Educ.* **1998**, *75* (12), 1580.
(30) Rajchakit, U.; Limpanuparb, T. Greening the Traffic Light: Air Oxidation of Vitamin C Catalyzed by Indicators. *J. Chem. Educ.* **2016**, *93* (8), 1486−1489.